

Screening and docking molecular studies of natural products targeting overexpressed receptors HER-2 in breast cancer

Abstract

The first cancer to strike a community is breast cancer. Because of its extremely high mitotic activity, breast cancer that tests positive for HER 2 is thought to have a bad prognosis. Due to the effects caused by chemical drugs, patients are increasingly turning to natural medicine, such as phytotherapy and nutritherapy. The main objective of this study is to search, using a bioinformatics approach (molecular docking), for new non-toxic anti-cancer inhibitors by carrying out a screening of 102 ligands from natural and dietary compounds, likely to interact with the HER-2. The results of the virtual screening permit to choose 23 best compounds which can be proposed as the best inhibitors of HER-2. Lycopene would be a very promising ligand which presents a DeltaG of -9.82 kcal/mol, followed by Beta-carotene (DeltaG of -8.58), P-cumaric acid kcal/mol (DeltaG of -8.57) and Curcumin (DeltaG of -8.46). Another compounds; luteolin, anacardium (Anacardic acid) and alpha-Tocopherol were found to have the strongest inhibitory effects, with DeltaG values of -7.92 kcal/mol, -7.89 kcal/mol and -7.85 kcal/mol, respectively, and act directly on residues keys found in the hydrophobic pocket II (ATP binding site) and the hydrophobic region (the α C- β 4 loop) of the EGFR domain. Pinoresino, Kaempferol and Caffeic acid with DeltaGs of -7.48 Kcal/mol, -6.88 Kcal/mol and -6.34 kcal/mol, and are three ligands specific to the conserved regions of the HER-2 receptor and interact with the tail respectively; C-terminal, the C-lobe activation loop and the N-lobe P loop of the tyrosine kinase domain. The comparison of Lapatinib (chemical compound) and **quercetin** (natural compound) have respectively DeltaG of -7.58 kcal/mol and -7.28 kcal/mol, form a hydrogen bond with the same residue of the hydrophobic region. All the natural molecules seem very promising and, after *in vitro/in vivo* tests, could constitute good substitutes for the chemotherapies currently used to treat breast cancers as well as other cancers.

Keywords: Brest cancer, HER-2, Molecular docking, Natural compounds

31

32 1. Introduction

33 After lung cancer, breast cancer is the most common malignancy in women and the
34 second leading cause of cancer-related deaths (1). The World Health Organization (WHO)
35 announced in early 2020 that the incidence of breast cancer is rising in developing nations as a
36 result of rising life expectancies, increased urbanization, and adoption of western lifestyles. It
37 is estimated that 627,000 women died of breast cancer in 2020, accounting for 15% of all female
38 cancer deaths.

39 Estrogen and progesterone hormone receptor dysfunction is typically associated with
40 breast tumors (2,3) Furthermore, a great deal of research has been done on the overexpression
41 of the human epidermal growth factor receptor 2 (HER2), EGFR1 (overexpression of the
42 epidermal growth factor receptor), and PI3Ka (dysregulation of the ER+ and ER-) signaling
43 pathways in breast cancer (3,4) Therefore, it is essential to continue discovering novel
44 techniques and compounds that target these proteins. Roughly 20% to 25% of all breast cancers
45 were caused by the transmembrane protein receptor known as human epidermal growth factor
46 receptor 2 (HER2), which is encoded by the HER2 gene located on chromosome 17 long arm.
47 The EGFR family, which consists of the four HER receptors HER4, HER3, HER2, and HER1,
48 includes HER2 (5). Specific tyrosine kinase residues are phosphorylated and signaling proteins
49 are activated upon HER2 receptor activation, which leads to the start of downstream signaling
50 processes. Apoptosis, angiogenesis, cell proliferation, and survival are all regulated by the
51 critical pathways induced by the HER2 receptor, which include the mitogen-activated protein
52 kinase (MAPK) and phosphatidylinositol triphosphate kinase (PI3K) signaling mechanisms (6).
53 In HER2+ breast cancers, overexpression of the HER2 receptor is known to be a HER2
54 activation mechanism. HER2-positive breast cancer remains a case study to this day. It is
55 considered a cancer with a poor prognosis due to its high mitotic activity and ability to
56 metastasize more easily. However, improved molecular genetic techniques have made it
57 possible to study resistance to the administration of trastuzumab (HERCEPTIN) and generate
58 new anti-HER2 targeted therapies. The monoclonal antibody pertuzumab and the tyrosine
59 kinase inhibitor lapatinib specifically target HER2 receptors. The adverse effects of these two
60 chemical and synthetic drugs include alopecia, nausea, vomiting, fatigue, fever, infection,
61 diarrhea, muscle pain, paresthesia, cognitive disorders, cardiotoxicity, leukemia,
62 gastrointestinal and dermatological reactions. Another several market drugs such as tamoxifen,

raloxifene, toremifene, and fulvestrant for the treatment of breast cancer are available, but each has its limitations, which cause irreversible side effects (7). The recent search is on for other, less toxic and natural molecules. Patients are therefore increasingly turning to natural medicine, such as phytotherapy and nutritherapy. There are various benefits to using natural products in the food and medicine development industries, such as their superior chemical diversity, biological potency, and structural complexity and optimize the regulation of natural product biosynthesis. Therefore, this study aimed to discover, *in silico*, a more selective natural compound targeting breast cancer for using as a therapeutic agent.

2. Material and Methods

2.1. Preparation of the protein

The crystal structure of the kinase domain of human HER2 was obtained from Protein Data Bank (PDB) (<https://www.rcsb.org>) (8), with PDB ID: 3PP0 (9). The structure was downloaded in .pdb format and was further prepared for the docking process.

2.2. Preparation of ligands

After an extensive literature search, 102 molecules that could have a positive interaction with the ErbB2 receptor tyrosine kinase domain in HER2+ breast cancer and that are derived from plants, microorganisms or food sources were selected. The ligand codes were obtained from PubChem (<https://pubchem.ncbi.nlm.nih.gov/>)(10), and Zinc Database (<https://zinc.docking.org/>) (11).

2.3. Pharmaco-toxicity study of ligands

In order to test the toxicity of the plant-derived molecules, we used the PKCSM Database online server (<http://structure.bioc.cam.ac.uk/pkcsm>) (12). The ligand codes obtained from PubChem and Zinc Database were copied to pkCSM Database to eliminate toxic ligands based on the following criteria : AMES toxicity, hERG K⁺ channel inhibitors toxicity and Hepatotoxicity.

2.4. Molecular docking

Molecular docking was performed by the SwissDock server (<http://www.swissdock.ch/>) (13), which allows importing the target molecule "tyrosine kinase domain of the HER2 receptor" and the ligands in purpose of testing their interactions, with the aim of studying the interactions of

94 these two molecules. Investigating the outcomes enables the identification of the binding
95 energy, the hydrogen bonds formed as well as the amino acids involved in these interactions.

96

97

98

99 **2.5. Docking results visualisation**

100 The visualisation of the molecular docking results from the SwissDock server is done using the
101 UCSF Chimera software (<https://www.cgl.ucsf.edu/chimera/>) (14) .

102

103 **3. Results and discussion**

104 **3.1. Ligand toxicity analysis**

105 Initially, 102 natural compounds were obtained from the databases. These molecules
106 can be found in food sources ; in plants or microorganisms. Some compounds were screened
107 for their toxicity based on the predicted results of the mutagenicity screening (AMES Toxicity),
108 HERG K⁺ channel inhibitor toxicity and hepatotoxicity. The results revealed that eight ligands
109 are potentially toxic (**Table 1**). This toxicity could be kept by decreasing the administrated
110 dose, respectively 0.558 log mg/kg/day, 0.36 log mg/kg/day, 0.654 log mg/kg/day, 0.144 log
111 mg /kg/day, 0.82 log mg/kg/day for the ligands Genipin, Sauchinone , Denbinobin, Xenognosin
112 and Kaempferol.

113

114

Table 1: Toxicity parameters of some compounds.

Molecules	Mutagenicity	K⁺ hERG 1	Na⁺ + hERG 2	Hepatotoxicity
Genipin	Yes	No	No	No
Sauchinone	Yes	No	No	No
Denbinobin	Yes	No	No	No
Furanodiene	No	No	No	No
Chalcones	No	No	No	No
Isoliquiritoside	No	No	No	No
Xenognosin	Yes	No	No	No
Kaempferol	Yes	No	No	No
Luteolin	Yes	No	No	No

Silibinin	Yes	No	Yes	No
Daidzeine	Yes	No	Yes	No

115

116

117

118 3.2. Interaction of ligands with HER2

119 In this study, the interaction of the 3PP0 protein against 84 ligands was investigated.

120 The results are shown in Tab.2.

121

122 **Table 2:** docking results of total ligands with the tyrosine kinase domain obtained by
123 Swissdock.

Ligands	Residue (s) target(s)	Length of hydrogen bond (Å°)	Interraction energy (kcal/mol)
Crocetin	ALA 706 ALA 706	3.011 3.324	-9.46
Secoisolariciresinol diglucoside	GLU 757	1.841	-8.41
Lycopene	-----	No hydrogen bond	-9.82
P-coumaric acid	-----	No hydrogen bond	-8,57
Curcumin	-----	No hydrogen bond	-8.46
Pomiferin	-----	No hydrogen bond	-8.08
Formononetin	-----	No hydrogen bond	-8.07
Rosmarinic acid	-----	No hydrogen bond	-7.83
3,4-Dihydroxybenzoic	GLY 737	1.915	-6.22
4 P-hydroxybenzoique 1 acid	SER 779	2.213	-6.88
4 P-hydroxybenzoique 2 acid	-----	No hydrogen bond	-6.21
Gallic acid	VAL 777	2.517	-6.25
Gentisic acid	-----	No hydrogen bond	-6.93
Syringic acid	CYS 805	3.096	-6.51
Vanillic acid	VAL 777	2.191	-6.20
Catechines	VAL 777	3.187	-6.82

Epicatechines	GLN 943	1.819	-6.74
Biochanine A	LEU 726	3.347	-6.67
Ergostane	-----	No hydrogen bond	-6.18
Glycitein	-----	No hydrogen bond	-6.37
Daidzeine	VAL 777	2.114	-6.61
Genistein	CYS 947	1.995	-7.54
Malvidin	VAL 777	3.031	-7.32
Delphinidine	-----	No hydrogen bond	-6.70
Cyanidin	GLN 709 GLN 709	2.003 1.929	-7.00
Acetoxypinoresinol	-----	No hydrogen bond	-7.29
Pinoresinol	SER 728	2.523	-7.80
Hydroxytyrosol	ARG 849	2.215	-6.91
Tyrosol	ARG 849	2.129	-6.36
Secoisolariciresinol	-----	No hydrogen bond	-7.49
Enterodiol	PRO 945	2.169	-6.63
Enterolactone	-----	No hydrogen bond	-7.51
Capsaicin	-----	No hydrogen bond	-7.62

CAPE Caffeic-acid-phenethyl ester	-----	No hydrogen bond	-6.46
α-Linolenic acid	SER 728	3.160	-7,69
ChlorogenicHeriguard acid	GLN 943	2.140	-6.96
Ferulic acid	-----	No hydrogen bond	-7,37
Gingerol	-----	No hydrogen bond	-7,27
Petunidin	-----	No hydrogen bond	-7,03
Pelagronidine	GLY 778	2,052	-6,38
Homocastasterone	ASP838	2.716	-7.44
Cafeic	LEU1000	2.044	-6.71
Sinapic	CYS 805	2.052	-7.40
3-Hydroxybenzoic	-----	No hydrogen bond	-6.68
O-coumaric acid	-----	No hydrogen bond	-6.05
Diindolylmethane	-----	No hydrogen bond	-7,31
Naringenine	GLN943	1.841	-6.65
Indol 3-carbinol	-----	No hydrogen bond	-6.13
Kaempferol	ASP 863	3.572	-6.88

Dihydroresveratrol	-----	No hydrogen bond	-7.15
Resveratrol	-----	No hydrogen bond	-6.51
Sulforaphane	MET 801	3.708	-7.10
Myricetin	-----	No hydrogen bond	-7.03
Quercetin	ALA706 VAL 777	2.130 3.491	-7.28
Apigenin	CYS 947	2.064	-7.55
Luteolin	ALA 706 VAL 777	2.132 2.247	-7.92
Fisetin	VAL777	3.336	-6.55
Sauchinone	-----	No hydrogen bond	-6.83
Denbinobin	-----	No hydrogen bond	-7.01
Furanodiene	-----	No hydrogen bond	-6.82
Chalcone	-----	No hydrogen bond	-7.19
Lupane	-----	No hydrogen bond	-6.77
Genipin	VAL 777 VAL 777	2.696 3.142	-6.50
Opium	VAL777	2.054	-6.70
Pyocyanin	MET801	2.162	-7.65
Ginsenosol	ALA706	2.131	-6.34
Menthol	VAL777	2.329	-6.10

Urocanic acid	MET801	2.182	-6.49
Anthranilic acid	ALA706 ALA706	2.410 2.177	-7.54
Anacardic acid	CYS805	2.049	-7.89
Diosmetin	VAL777 GLN709	2.073 2.348	-6.60
Khahalalide D	THR759	2.385	-7.39
Alpha-tocopherol	MET801	2.433	-7.85
Beta-carotene	-----	No hydrogen bond	-8.58
Choline	CYS802	2.442	-6.30
Sesamol	MET801	2.612	-6.09
Silibinin	VAL777 LEU711	2.197 2.546	-7.16
Xanthoxylin	VAL777	2.509	-6.26
Isofraxidin	MET801 VAL777	2.084 2.117	-7.77
Phloretic acid	MET801 VALL777	1.939 2.034	-7.06
Indole-3-carboxylic acid	GLN990 PHE731 GLN990	2.118 2.003 2.077	-7.81
Garlic	-----	No hydrogen bond	-6.69
Xenognosin	MET801	2.156	-6.86

124

125

126 *3.3. Ligands interacting with conserved residues of the tyrosine kinase* 127 *domain of EGFR family receptors.*

128 It note that there are 47 complexes formed between the ligands and the tyrosine kinase domain
129 of 3PP0 that have the lowest score energies compared to the other ligands by forming hydrogen
130 bonds with essential residues conserved in the EGFR family (see Table 2).

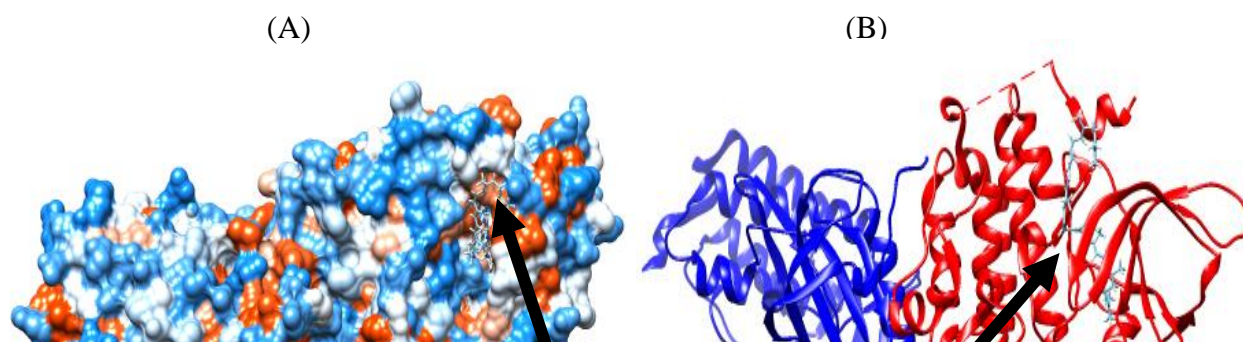
131 Therefore, the best ligand according to the interaction energy is represented by Lycopene
132 **Tab.2.** As for Lycopene from tomato, it presents an interaction energy of -9.82 kcal/mol with
133 no hydrogen bonds were predicted by SwissDock suggesting the existence of other types of
134 bonds (**Fig.1**).

135

136

137

138



139
140
141
142
143
144
145
146
147
148
149
150
151
152
153
154
155
156
157
158
159
160
161
162
163
164
165
166
167
168
169
170
171
172
173
174
175
176
177
178
179
180

Figure.1 : Three-dimensional illustration of the 3PP0-Lycopene complex using the molecular surface (A) and the ribbon model (B)

Taking into account what has been cited in the literature including Met801 which is located in the Adenine region of the ATP binding site and Cys805 of hydrophobic pocket II, it has noted that some ligands form interactions with the ATP binding site (**Tab.2**) (**15**).

Compounds establishes a hydrogen bond with the residue Met 801 in the adenine region are as follow:

-**Alpha-Tocopherol** from sunflower oil has an interaction energy of -7.85 kcal/mol.

-**Isofraxidin** of the species *Eleutherococcus senticosus* known as Siberian ginseng has an interaction energy of -7.77 kcal/mol.

-**Pyocyanin**: a blue green phenazine molecule, produced specifically by the bacterium *Pseudomonas aeruginosa*, has an interaction energy of -7.65 kcal/mol.

-**Sulforaphane**, mainly found in broccoli and cabbage., has an interaction energy of -7.10 kcal/mol.

-**Phloretic acid** belongs to the class of organic compounds present in peanuts and avocados has an interaction energy of -7.06 kcal/mol.

-**Xenognosin** present in common peas *Pisum sativum* legumes, belongs to the class of organic compounds, presents an interaction energy of -6.86 kcal/mol.

-**Urocanic acid** essentially found in the fungus *Hippospongia communis* has an interaction energy of -6.49 kcal/mol.

-**Sesamol** of the sesame seed has an interaction energy of -6.09 kcal/mol.

The other compounds forming hydrogen bonds with cysteine residue 805 in the hydrophobic pocket II are: **Syringic acid** from olive oil and **Anacardic acid**, component of cashew nuts, present interaction energies (DeltaG) of -6.52 and -7.89 kcal/mol respectively.

These ligands interacting and forming hydrogen bonds with residues Met801 and Cys805 in the ATP binding site in the afore mentioned regions may have the potential to be competition inhibitors by blocking the access of ATP to its specific site on the tyrosine kinase domain (**16**, **17**). In this study the ligand with the best interaction energy value with the ATP binding site is **Anacardic acid** with DG of -7.89 kcal/mo (**Fig.2**).

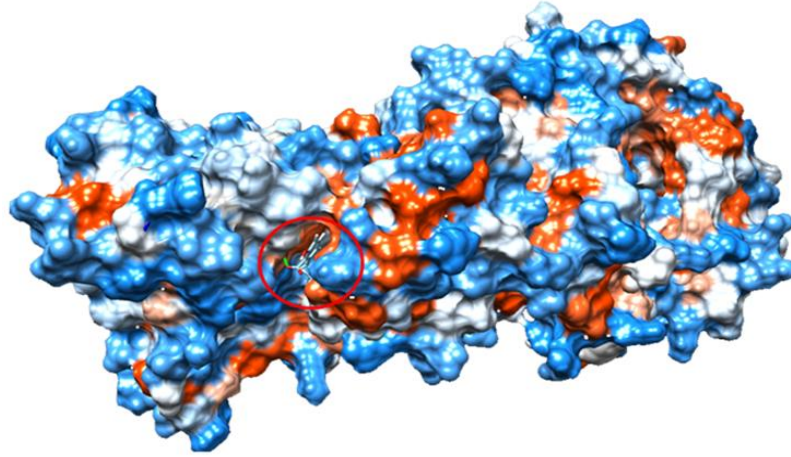


Figure.2: Three-dimensional illustration of the 3PP0 -Anacardic acid complex using the molecular surface.

Two olive oil ligands among the 21 ligands act on the N-lobe of the tyrosine kinase domain were selected according to their interactions with residues in the ($C\alpha$) helix span residues (729-744). **3,4-Dihydroxybenzoic acid** exhibits an interaction energy of -6.22 kcal/mol and establishes a hydrogen bond with the residue Gly737. **Sinapic acid** has an interaction energy of -7.40 kcal/mol and establishes a hydrogen bond with the residue Gly732.

Both ligands form hydrogen bonds, **3,4-dihydroxybenzoic acid** with residue Gly737 and **Sinapic acid** with residue Gly732 in the ($C\alpha$) helix extent. This could destabilize the active open conformation of the activation loop (C-helix-in-DFG-in), no binding of the ATP substrate on its specific site, blockage of trans-autophosphorylation of the activation loop which maintains its inactive conformation, the ATP binding groove is no longer accessible, the tyrosines of the C-terminal tail will not be phosphorylated by the catalytic loop. This induces blockage of the downstream signaling cascade **(18)**.

In the present study, the target with the best interaction energy value acting on the N-lobe ($C\alpha$ -helix) is **Sinapic acid** with a DG of -7.40 kcal/mol (**Fig.3**).

(A)

(B)

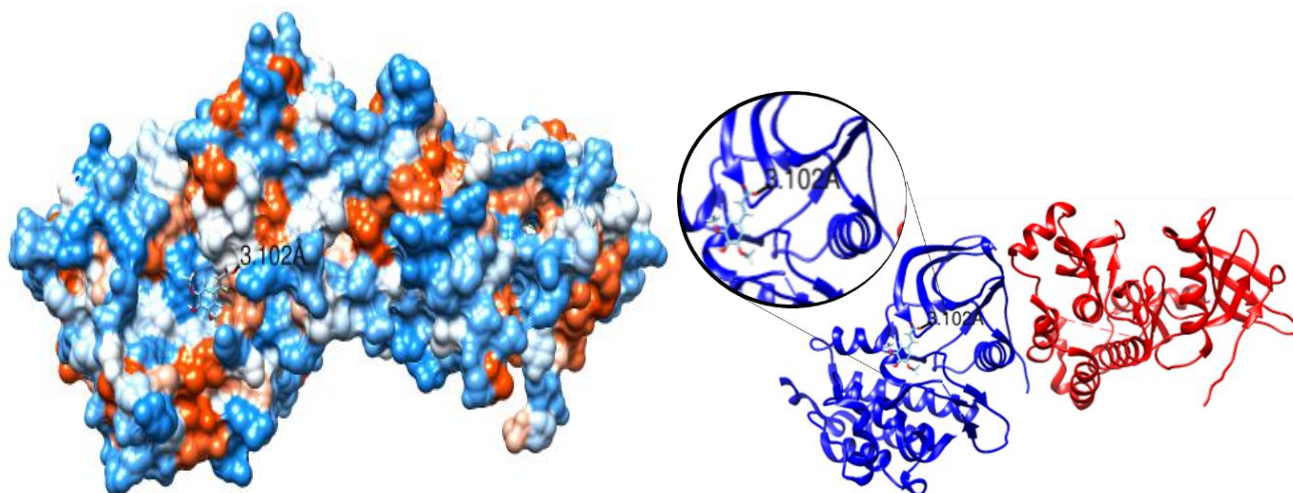


Figure.3: Three-dimensional illustration of the 3PP0 -Sinapic acid complex using the molecular surface (A) and the ribbon model (B)

203
 204
 205
 206
 207
 208
 209
 210
 211
 212
 213
 214
 215
 216
 217
 218
 219
 220
 221
 222
 223
 224
 225
 226
 227
 228
 229
 230
 231

Three of these 47 ligands act on the A-loop of the C-lobe of the tyrosine kinase domain. According to the literature, the 20-30 residue sequence of the activation loop (Asp831-Val852 in the EGFR family), which contains the conserved base DFG motif (Asp831-Phe-Gly833 in the EGFR family) and extends to an APE (Ala-Pro-Glu) motif, also contains the Tyr845 residue which is one of the target tyrosines for autophosphorylation by the catalytic loop (16, 17, 18).

-Tyrosol and **Hydroxytyrosol** of olive oil have interaction energies of -6.36 and -6.91 kcal/mol respectively and each establishes a hydrogen bond with an estimated length of 2.129 Å for tyrosol and 2.215 Å for hydroxytyrosol with the same residue Arg849 of the chain A for tyrosol and B for hydroxytyrosol.

-Homocasterone from beans has an interaction energy of -7.44 kcal/mol establishing a strong hydrogen bond with an estimated length of 2.716 Å with Asp838 of the A chain.

Thus the ligand **Homocasterone** forms a hydrogen bond with the residue Asp838, the ligands Tyrosol and Hydroxytyrosol, each form a hydrogen bond with the residue Arg849 of the activation loop. These ligands can therefore block its activation, its passage between the conformations, inactive (C-helix-out-DFGout) to the partially inactive conformation (C-helix-in-DFGout) and finally to the active conformation (C-helix-in-DFGin). This effect is possible by sequestering the trans autophosphorylation of these tyrosine residues to phosphotyrosines by the catalytic loop after dimerization. Thus the ATP binding groove is not accessible, no trans phosphorylation of the C-terminal tail and therefore no recruitment of adaptor proteins (16, 17, 18, 19, 20).

232 This study shows that the ligand with the best interaction energy value that acts on loop A and
233 lobe-C is **Homocasterone** with a DG of -7.44 kcal/mol (**Fig.4**).

234
235
236
237

238
239

240
241
242
243
244
245
246
247
248
249
250
251
252
253
254

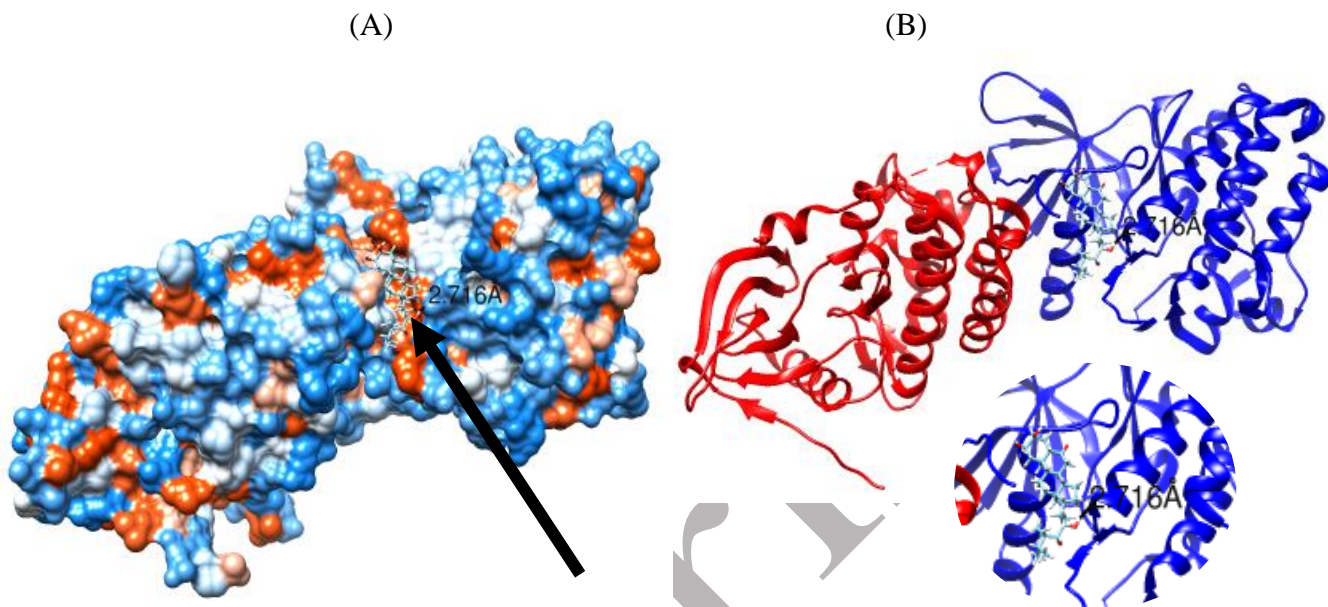


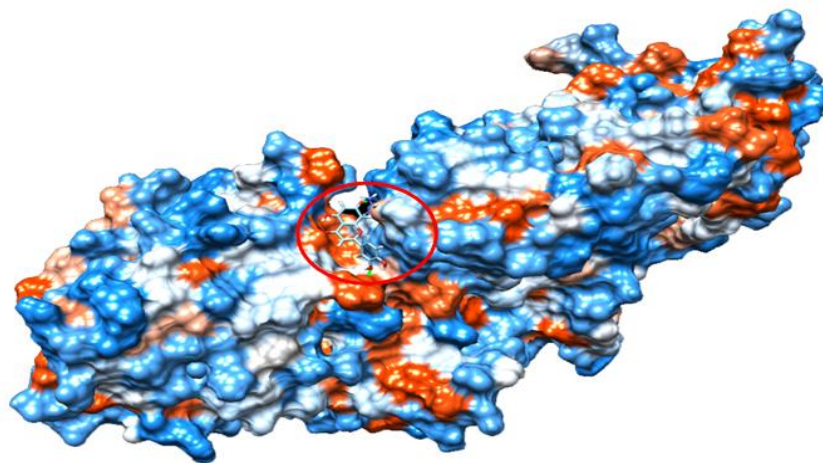
Figure.4: Three-dimensional illustration of the 3PP0 – Homocasterone complex using the molecular surface (A) and the ribbon model (B)

255
256
257

258
259 Other ligands were selected according to their interactions with residues in the hydrophobic
260 region of ErbB2 which includes the following residues: Val773, Met774, Gly776, Val777,
261 Gly778, and Val782 in the α C- β 4 loop (21). For exemple, **Pelagronidin** from grapes establishes
262 a hydrogen bond with Gly778.

263 *Sixteen of these ligands establish a hydrogen bond with the same Val777 residue (**Tab.2**) :
264 **Vanillic acid** from olive oil , **Catechin** from blackcurrant, **Malvidin** from grapes, **Fisetin** from
265 strawberries and apples, **Genipin** of the *Gardenia Jasminoides Ellis* species , **Opuim**, **Gallic**
266 **acid**, **Menthol** from peppermint and tea, **Diosmetin** from sage, thyme, **Quercetin** from red onions
267 or buckwheat, **Luteolin** from green peppers, olive oil and carrots, **Xanthoxylin** from fats and
268 oils, herbs and spices, **Isofraxidin** **Phloretic acid**, **Silibinin** extracted from the milk thistle
269 flower and **Daidzein** present in flax seeds,. Although these two ligands have a better interaction
270 energy and strong bonds but according to the Pharmaco-toxicity test of the ligands showed that
271 these 2 molecules have a mutagenic power therefore are toxic molecules.

272
273 Indeed these ligands forming hydrogen bonds with the residues (valine777) which belong to
274 the hydrophobic region of ErbB2 (α C- β 4 loop) and which interact with the activation loop, can
275 destabilize these conformational changes, of the inactive conformation (C- helix-out-DFGout),
276 to the partially inactive conformation (C-helix-in-DFGout) and finally to the active
277 conformation (C-helix-in DFGin). This by sequestering its trans autophosphorylation by the
278 catalytic loop after dimerization. Thus the ATP binding groove remains covered, no trans
279 autophosphorylation of the C-terminal tail and therefore no recruitment of adapter proteins (21).
280 This results indicated that the ligand which has the best interaction energy value interacts with
281 the residues of the hydrophobic region in the loop (α C- β 4) is **Luteolin** with a DG of -7.92
282 kcal/mol (Fig.5).



283
284 **Figure.5.** Three-dimensional illustration of the 3PP0 -Luteolin complex using the molecular
285 surface.
286 According to the literature the residues of the hydrophobic region of loop A are Iso861, Thr862,
287 Phe864, Leu866 and Leu869. Only the shared interaction between the two active and inactive
288 conformations that takes place between Ser783 with in the hydrophobic region of ErbB2 (α C-
289 β 4 loop) and residue Iso861 of loop A allows the interaction between the latter and the α C- β 4
290 loop (21).
291 Thus the ligands **Vanillic acid, Catechins, Malvidin, Fisetin, Genipin, Pelagronidin and 4**
292 **p-hydroxybenzoic acid**, forming hydrogen bonds with residues belonging to the hydrophobic
293 region of ErbB2 (α C- β 4 loop) and interacting with the activation loop, can destabilize these
294 conformational changes from the inactive conformation (C-helix-out-DFGout), to the partially
295 inactive conformation (C-helix-in-DFGout) and finally to the active conformation (C-helix-in-
296 DFGin), this by sequestering its trans autophosphorylation by the catalytic loop after

297 dimerization. Thus the ATP-binding groove remains covered with no trans autophosphorylation
298 of the C-terminal tail and so no recruitment of adaptor proteins (21).

299 In this study the ligand that has the best interaction energy value interacts with residues in the
300 hydrophobic region (in the C α - β 4 loop) is **malvidin** with a DG of -7.32 kcal/mol (Fig.6).

301

302 (A)

303

304

305

306

307

308

309

310

311

312

313

314

315

316

317

318

319

320

321

322

323

324

325

326

327

328

329

330

331

332

333

334

335

336

337

338

339

340

(B)

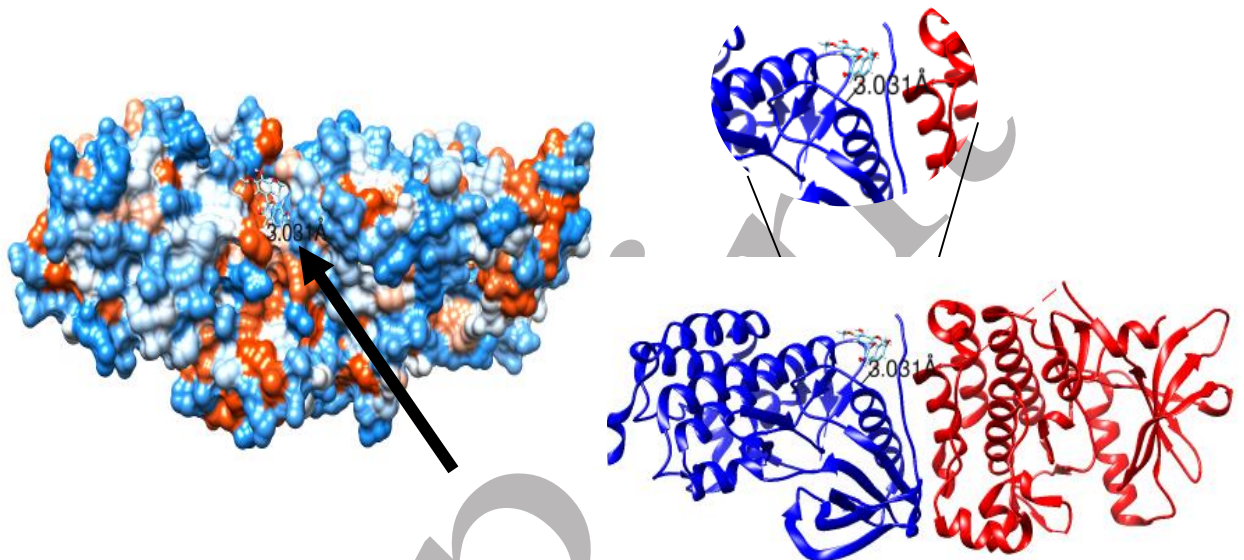
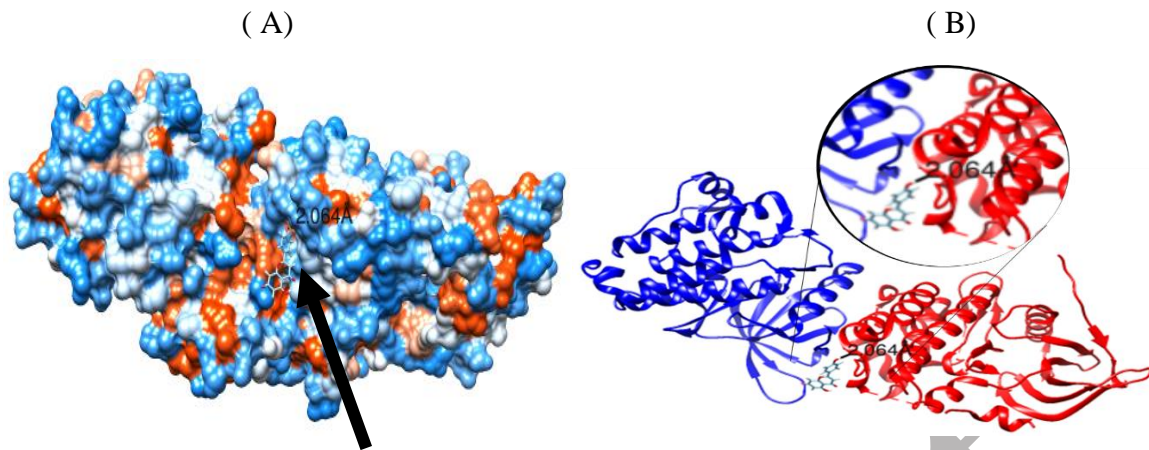


Figure 6: Three-dimensional illustration of the 3PP0 -Malvidin complex using the molecular surface (A) and the ribbon model (B)

327 The remaining five ligands were selected according to their interactions with residues that lie
328 between the tyrosines of the C-terminal tail (Tyr874, Tyr992, Tyr1048, Tyr1068, Tyr1086,
329 Tyr1101 and Tyr1173) (Tab.2) (17). The previously mentioned tyrosines correspond to
330 residues trans-autophosphorylated by the catalytic loop so ligands that form hydrogen bonds,
331 **Epicatechin** and **Naringenin** with residue Gln943, **Apigenin** with residue Cys947, **Genistein**
332 with residue Cys947, that lie between these tyrosines may be susceptible to sequester at the
333 interaction of the C-terminal tail with the catalytic loop. Therefore the tyrosines will not be
334 trans-autophosphorylated and thus no recruitment of the adaptor proteins (17).

335 The ligand that has the best interaction energy value with residues that lie between the tyrosines
336 of the C-terminal tail is **Apigenin** with a DG of -7.55 kcal/mol (Fig.7).

337



338

339

340

341

342

343

344

345

346

347

348

349

Figure 7 : Three-dimensional illustration of the 3PP0- Apigenin complex using the molecular surface(A) and the ribbon model (B)

3.4. Ligands interacting with specific residues of the HER-2 receptor tyrosine kinase domain.

One ligand acts on the P-loop of the N-lobe of the tyrosine kinase domain non-conserved in the EGFR family and specific for HER2 were selected in relation to their interaction with the residues in the extent (from residue Leu726 to residue Val734) (9). **Pinoresinol** from olive oil has an interaction energy of -7.48 kcal/mol and establishes a strong hydrogen bond whose length is estimated at 2.613 Å with the residue Ser728 (Fig.8). This ligand establishes a hydrogen bond with the P-loop, which can destabilize the open active conformation of the activation loop (C-helix-in-DFGin), not binding the ATP substrate to its specific site. This induces the blocking of the downstream signaling cascade (16).

350

351

352

353

354

355

356

357

358

359

360

361

362

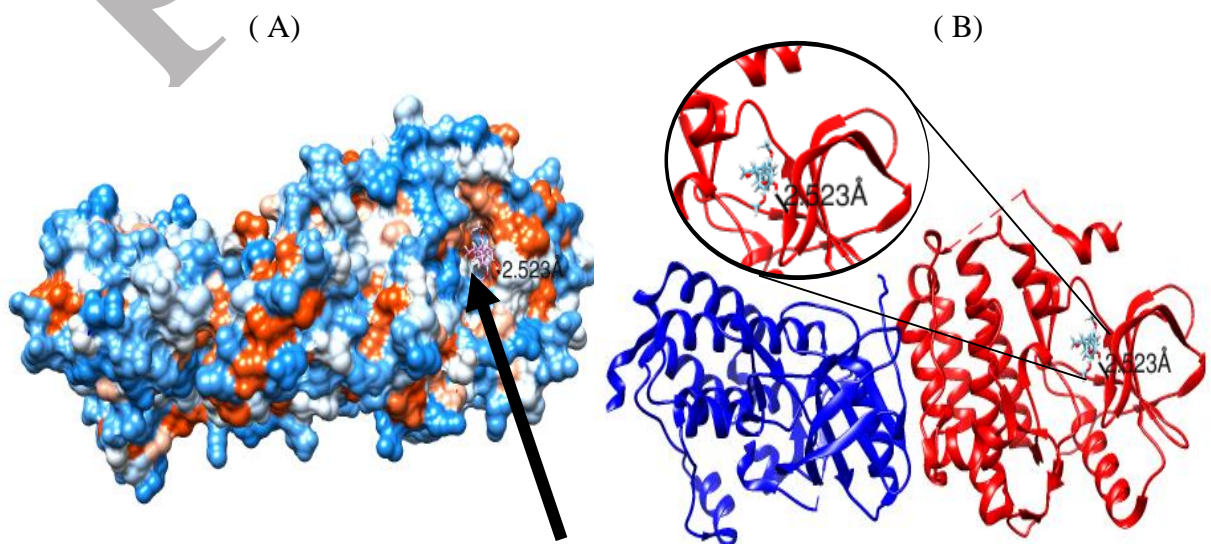
363

364

365

366

367



372
373
374
375
376
377
378
379
380
381
382
383
384
385
386
387
388
389
390
391
392
393
394
395
396
397
398
399
400
401

Figure 8. Three-dimensional illustration of the 3PP0-Pinoresinol complex using the molecular surface (A) and the ribbon model (B)

One ligand acts on the C-terminal tail of the non-conserved tyrosine kinase domain in the EGFR family and specific for HER2 was selected based on its interaction with the residues in the extended (from residue Pro999 to residue Leu1009) : **The caffeic acid** of olive oil has an interaction energy of -6.71 kcal/mol established a hydrogen bond whose length is estimated at 2.044Å with the residue **Leu1000 (9)**.

There were two ligands, acting on the P-loop of the N-lobe of the tyrosine kinase domain selected according to their interaction with residues in the sequence extending from residue Leu726 to residue Val734 (9). **Biochanin A** from Soybean has an interaction energy of -6.67kcal/mol with Leu 726 **and α-Linolenic** acid from soybean, presents interaction energie of -7.69 kcal/mol and a strong hydrogen bond with an estimated length of 3.160Å with the residue Ser728.

The Cα-helix and P-loop are in close proximity and interact with ATP required for trans-autophosphorylation in the ATP binding site (9, 17). The ligands **Biochanin A, Pinoresinol** and **α-Linolenic** acid form hydrogen bonds with the P-loop, can destabilize the active open conformation of the activation loop (C-helix-in-DFGin) thus no ATP substrate binding at its specific site which induces blockage of the downstream signaling cascade (18).

The ligand that has the best interaction energy value with the N-lobe P-loop residues specific for HER2 is **α-Linolenic** with a DG of -7.69 kcal/mol (Fig. 9).

(A)

(B)

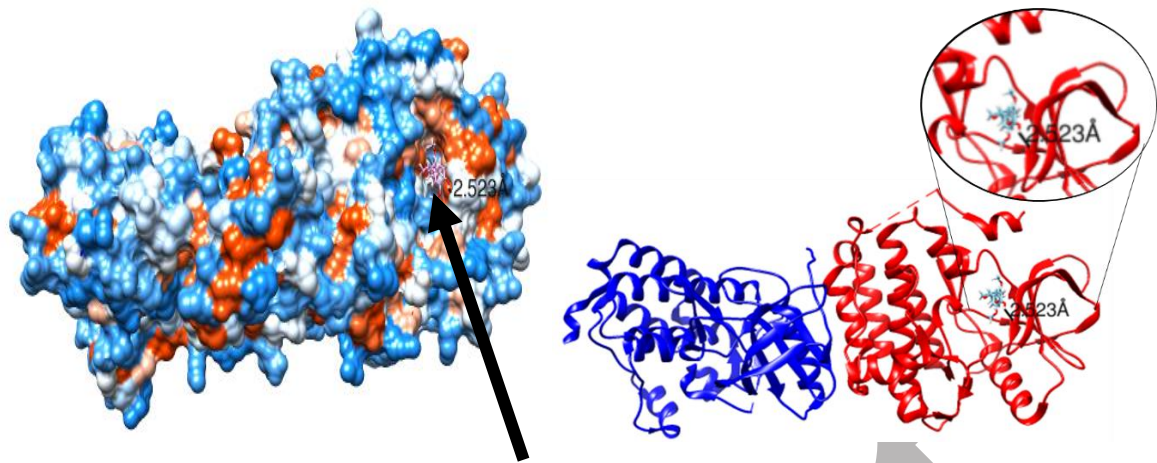


Figure 9. Three-dimensional illustration of the 3PP0 - α -Linolenic complex using the molecular surface (A) and the ribbon model (B)

402

403

404

405

406

407

408

409

410

411

412

413

414

415

416

417

418

419

420

421

422

423

424

425

426

427

428

429

430

431

432

As for the remaining ligand acting on the helix ($C\alpha$) of the N-lobe of the tyrosine kinase domain was selected according to its interaction with the residues in the stretch of the sequence extending from residue Pro761 to residue Ala775.

One ligand acts on the C-lobe activation loop of the HER2 receptor-specific domain tyrosine kinase domain was selected based on their interaction with residues spanning Asp863 to Val884 with the DFG motif (from residue Asp863 to residue Gly865) : **Kaempferol** Present an interaction energy of **-6.88 Kcal/mol** establishes a hydrogen bond whose length is estimated at 3.572 Å with the residue ASP863 (**Fig.10**).

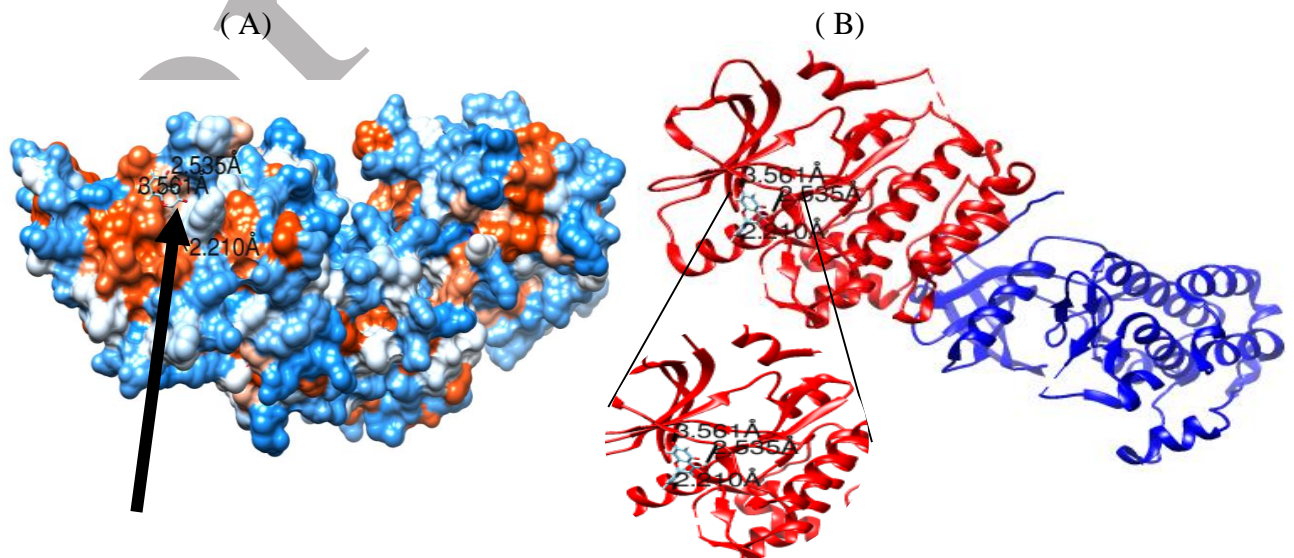


Figure 10. Three-dimensional illustration of the 3PP0 - Kaempferol complex using the molecular surface (A) and the ribbon model (B)

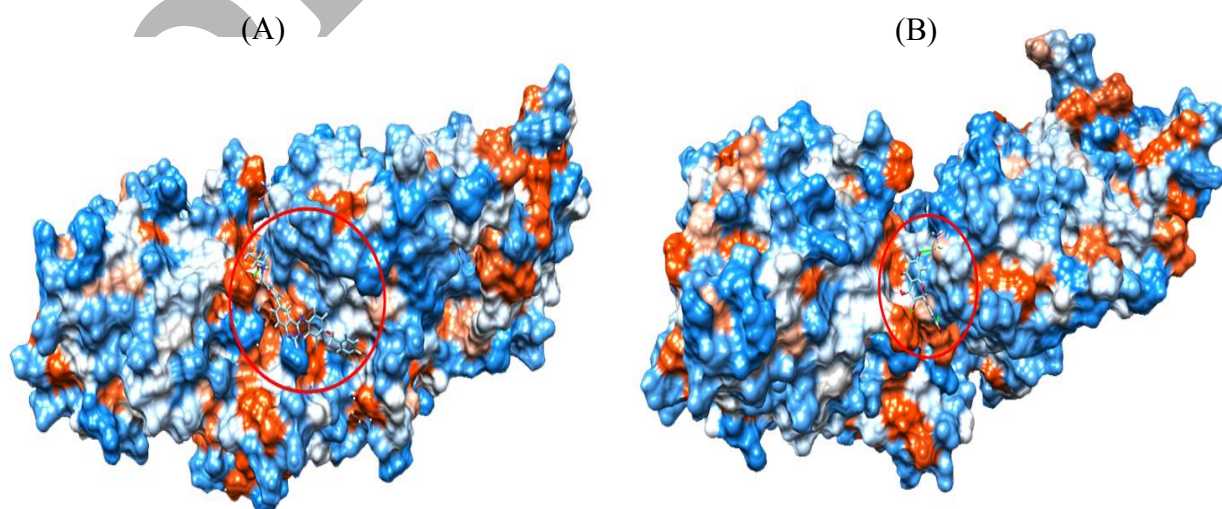
3.5. Visualization of Lapatinib Docking Results with 3PP0

Lapatinib is a ligand used as a chemical treatment in HER2+ breast cancer that is specific for inhibiting protein tyrosine kinase signaling pathways (22). Our results indicate that it has an interaction energy of -7.58 kcal/mol and establishes a hydrogen bond whose length is estimated at 2.303Å with the Val777 residue of the A chain. Lapatinib therefore interacts with the residues of the hydrophobic region of ErbB2 in the α C- β 4 loop (Fig.11 A).

3.6. Comparison of the two ligands Lapatinib and Quercetin

The quercetin of red onions or buckwheat, has an interaction energy of -7.28 Kcal/mol establishes a hydrogen bond whose length is estimated at 2.130 Å with the residue Val777 (Fig.11 A).

Based on the visualization of the results of the two ligands, Lapatinib and quercetin, of which the first constitutes a modified chemical ligand and the second is a natural ligand coming mainly from red onions, it appears that : each of the two establishes a hydrogen bond of different lengths, of 2.303Å for Lapatinib and of 2.130Å for a quercetin , with the same residue valine777 of the hydrophobic region (in the α C- β 4 loop), with different energies of interaction, -7.58kcal/mol for Lapatinib and -7.28kcal/mol for quercetin . Certainly, Lapatinib has a better interaction energy but remains as molecules of chemical origin which has its side effects, as for quercetin, in addition to its possible inhibition of 3PP0 has other beneficial effects on health.



468 **Figure 11.** Three-dimensional illustration of the 3PP0 - Lapatinib (A) and 3PP0 - meletin
469 (B) using the molecular surface
470

471
472 Indeed, quercetin or vitamin 'P' is a food-derived compound, a bioflavonoid, found in the
473 pigments of colored fruits and vegetables, such as red onions, spinach, turmeric, apples, red
474 grapes, carrots, berries, broccoli, green tea, lovage, but also chocolate or red wine. It is a natural
475 antioxidant, helps fight against oxidative stress by capturing and blocking the activity of free
476 radicals, but also by inhibiting the oxidation of lipids. It is also involved in the regulation of
477 signaling pathways, cell cycle proliferation and the immune response.

478
479 In summary, investigating *in silico* before proceeding to the experimental stage can save a
480 great deal of time and money. A number of ADMET factors, toxicological effects, and the likely
481 active medication can all be predicted with the use of *in silico* technologies. The oral
482 bioavailability of drugs was predicted using a number of prediction methodologies in this study,
483 which may open the door to the creation of safer, innovative pharmaceuticals. Upon analyzing
484 the screening and molecular docking studies, we reported that a large number of natural product
485 could be employed as potential HER2 antagonists for the treatment of breast cancers. Additional
486 wet-lab research is necessary to further evaluate these selected compounds.

487 **Authors' Contribution**

488 Conceived and designed experiments: Nesrine Lenchi

489 Conducted experiments: Nesrine Lenchi

490 Analyzed data: Nesrine Lenchi, Naima Maouche, Souad Khemili-Talbi.

491 Wrote the paper: Nesrine Lenchi

492 **Data Availability**

493 The data that support the findings of this study are available on request from the corresponding author.

494 **Ethics**

495 The authors have observed all ethical points including non-plagiarism, double publication, data
500 distortion and data manipulation in this article.

501 **Conflict of Interest**

502 The author declares no known competing interest.

503 **References**

- 006 1. Domeyer PJ, Sergentanis TN (2020). New Insights into the Screening, Prompt
007 Diagnosis, Management, and Prognosis of Breast Cancer. *J Oncol.*:8597892. doi:
008 10.1155/2020/8597892. PMID: 32308682; PMCID: PMC7142357.
- 009 2. Dai X, Xiang L, Li T, Bai Z (2016). Cancer hallmarks, biomarkers and breast cancer
010 molecular subtypes. *Cancer J.*:7:1281-1294.
- 011 3. Hsu JL, Hung M-C (2016). The role of HER2, EGFR, and other receptor tyrosine kinases
012 in breast cancer. *Cancer Metastasis Rev.*;*35*:575-588.
- 013 4. Maennling AE, Tur MK, Niebert M, et al. (2019). Molecular targeting therapy against
014 EGFR family in breast cancer: progress and future potentials. *Cancers.*;*11*:1826.
- 015 5. Schlam I, Swain SM (2021). HER2-positive breast cancer and tyrosine kinase inhibitors:
016 the time is now. *NPJ Breast Cancer.*;*7*:56-12.
- 017 6. Furrer D, Paquet C, Jacob S, Diorio C (2018). The human epidermal growth factor
018 receptor 2 (HER2) as a prognostic and predictive biomarker: molecular insights into
019 HER2 activation and diagnostic implications. *Cancer Progn.*
020 doi:10.5772/intechopen.78271.
- 021 7. Sharma D, Kumar S, Narasimhan B (2018). Estrogen alpha receptor antagonists for the
022 treatment of breast cancer: a review. *Chemistry Central Journal.*; 12(1):107.
023 <https://doi.org/10.1186/s13065-018-0472-8> PMID: 30361894
- 024 8. Berman HM, Westbrook J, Feng Z, Gilliland G, Bhat TN, Weissig H, Shindyalov IN,
025 Bourne PE (2000). The Protein Data Bank *Nucleic Acids Research* 28: 235-
026 242 <https://doi.org/10.1093/nar/28.1.235>.
- 027 9. Aertgeerts K, Skene R, Yano J, Sang BC, Zou, H, Snell G, Jennings A, Iwamoto K,
028 Habuka N, Hirokawa A, et al. (2011) Structural analysis of the mechanism of inhibition
029 and allosteric activation of the kinase domain of HER2 protein. *J. Biol. Chem.*, 286,
030 18756–18765.
- 031 10. Kim S, Chen J, Cheng T, Gindulyte A, He J, He S, Li Q, Shoemaker BA, Thiessen PA,
032 Yu B, Zaslavsky L, Zhang J, Bolton EE. PubChem 2023 update. *Nucleic Acids Res.* 2023
033 Jan 6;51(D1):D1373-D1380. doi:10.1093/nar/gkac956.
- 034 11. Irwin JJ, Sterling T, Mysinger MM, Bolstad ES, and Coleman RG (2012). ZINC: A Free
035 Tool to Discover Chemistry for Biology. *Journal of Chemical Information and*
036 *Modeling* 52 (7), 1757-1768 DOI: 10.1021/ci3001277.
- 037 12. Pires DE, Blundell TL, Ascher DB (2015). pkCSM: Predicting Small-Molecule
038 Pharmacokinetic and Toxicity Properties Using Graph-Based Signatures. *J Med Chem.*
039 ;58(9):4066-72. doi: 10.1021/acs.jmedchem.5b00104. Epub 2015 Apr 22. PMID:
040 25860834; PMCID: PMC4434528.
- 041 13. Grosdidier A, Zoete V, Michielin O (2011). SwissDock, a protein-small molecule
042 docking web service based on EADock DSS, *Nucleic Acids Research*, Volume 39, Issue
043 suppl_2, 1 July, Pages W270–W277, <https://doi.org/10.1093/nar/gkr366>.
- 044 14. Pettersen EF, Goddard TD, Huang CC, Couch GS, Greenblatt DM, Meng EC, Ferrin TE.
045 (2004) [UCSF Chimera--a visualization system for exploratory research and analysis.](https://doi.org/10.1093/nar/gkr366) *J*
046 *Comput Chem.* (13):1605-12.
- 047 15. Yim-im, W, Sawatdichaikul O, Semsri S, Horata N, Mokmak W, Tongsimma S,
048 Suksamrarn A , & Choowongkomon K (2014). Computational analyses of curcuminoid
049 analogs against kinase domain of HER2. *BMC Bioinformatics*, 127063, 1–13.
- 050 16. Aller P. (2004). Etude Du domaine transmembranaire de recepteur tyrosine kinase dans
051 un environnement membranaire. Aspects structuraux et mecanistiques explores par
052 dynamique moleculaire : *HAL Id : tel-00009393*.
- 053 17. Martin-Fernandez, ML, Clarke DT, Roberts SK, Zanetti-Domingues LC, & Gervasio F
054 L (2019). Structure and Dynamics of the EGF Receptor as Revealed by Experiments and

- 000 Simulations and Its Relevance to Non-Small Cell Lung Cancer. *Cells*, 8(4),
006 316.<https://doi.org/10.3390/cells8040316>.
- 007
008 18. Modi V & Dunbrack RL (2019). Defining a new nomenclature for the structures of active
009 and inactive kinases. *Proceedings of the National Academy of Sciences of the United*
010 *States of America*, 116 (14), 6818–6827. <https://doi.org/10.1073/pnas.1814279116>.
- 011
012 19. Vijayan RSK, He P, Modi V, Duong-Ly KC, Ma H, Peterson JR, Dunbrack RL & Levy
013 RM (2015). Conformational analysis of the DFG-out kinase motif and biochemical
014 profiling of structurally validated type II inhibitors. *Journal of Medicinal Chemistry*,
015 58(1), 466–479. <https://doi.org/10.1021/jm501603h>.
- 016
017 20. Klug LR, Kent JD & Heinrich MC (2018). Structural and clinical consequences of
018 activation loop mutations in class III receptor tyrosine kinases. *Pharmacology and*
019 *Therapeutics*, 191: 123–134. <https://doi.org/10.1016/j.pharmthera.2018.06.016>
- 020
021 21. Shih AJ, Telesco SE, & Radhakrishnan R (2011). Analysis of somatic mutations in
022 cancer: Molecular mechanisms of activation in the ErbB family of receptor tyrosine
023 kinases. *Cancers*, 3(1), 1195–1231. <https://doi.org/10.3390/cancers3011195>
- 024
025 22. Ulrich L, Okines AF (2021). Treating Advanced Unresectable or Metastatic HER2-
026 Positive Breast Cancer: A Spotlight on Tucatinib. *Breast Cancer (Dove Med*
027 *Press)*.;13:361-381 <https://doi.org/10.2147/BCTT.S268451>.
- 028
029
030